Journal of Geological Resource and Engineering 6 (2018) 135-142
doi:10.17265/2328-2193/2018.04.001

The Response of a Shear Beam as 1D Medium to Seismic Excitations Dependent on the Boundary Conditions

Aleksandra Risteska and Vlado Gicev

Department of Applied Mathematics, Faculty of Computer Science, University "Goce Delcev", Stip 2000, R. Macedonia

Abstract: We study response of a shear beam to seismic excitations at its base. The research is conducted using computer simulation of the wave propagation on a numerical model. The wave equation is solved using the method of finite differences (FD) where the spatial and temporal derivatives are approximated with FD. We used formulation of the wave equation via the particle velocities, strains, and stresses. Integrating particle velocities in time, we obtained displacements at spatial points. The main goal in this research is to study phenomena occurring due to three different types of boundary conditions, Dirichlet, Neumann, and moving boundary when simple half-sine pulse propagates through 1D medium modeled as a shear beam.

Key words: Wave propagation, particle velocity, stress, strain, boundary conditions, numerical simulation.

1. Introduction

In the problems dealing with infinite region, as the wave propagation problems in seismology, it is impossible and useless to model the whole region. Instead, we model and study only one part of the whole region, the region of interest. To analyze only one part of the whole region we need to utilize so called artificial boundaries [1, 2]. They are not physical boundaries, but artifacts used to simulate wave propagation outside of the numerical model.

Opposite of the problems dealing with wave propagation in infinite domain, there is a wide research field in the earthquake engineering treating response of structures with finite dimensions to seismic excitations. In this problem, the boundaries bounding the structure are physical or real. In this case, the response of the structure inside depends upon the solution at the boundaries. Different boundary conditions imply different response of same structure excited by same excitation.

Corresponding author: Vlado Gicev, Ph.D., professor, research fields: earthquake engineering, numerical analysis.

To show the influence of the boundary conditions on the response of the structures, in this paper we study several aspects of the response of a simple shear beam (1D medium) model of a structure excited by simple half-sine pulse. Although the shear beam model is one of the simplest mathematical models of the real 3-D structures (buildings, bridges, chimneys, multilayered soil etc.), through numerical simulation on this model, many physical phenomena of the linear [3] and nonlinear [4, 5] response of the structure can be studied [6, 7]. Based on these studies we learned under what conditions, where, and when peaks of the response of the structure to seismic excitation occur [4, 8].

The boundaries occuring in wave propagation problems can be classified into three groups [9]:

- elementary (non-transmitting) boundaries;
- consistent (global) boundaries;
- imperfect (local) boundaries.

In this paper we study the features of the response due to three types of boundaries. First, we analyze the non-transmiting (totally reflecting) elementary boundaries. For that purpose we study two cases of shear beam model. In both cases, at the bottom end we

prescribe zero motion (Dirichlet boundary condition or fixed boundary). In the first case, at the top end of our shear beam model, we imply prescribed zero displacement (Dirichlet, fixed) boundary condition, while in the second case we imply prescribed zero derivative of displacement (Neumann, free-stress) boundary condition. In both cases, the boundaries are perfect reflectors, e.g. the wave energy is totally reflected from the boundaries into the inner region of the shear beam.

2. The Model

The model in this paper is a shear beam excited at its bottom by prescribed motion in form of half-sine pulse. After the motion is prescribed at the bottom, we take that the bottom end does not move and the displacement is zero during whole simulation. The shear beam is divided on *m* equal intervals (*m* = 200 in this paper). The governing equation of the problem is the wave equation implemented with numerical scheme in our model. This numerical scheme causes propagation of the prescribed half-sine pulse along the shear beam with velocity of propagation $\beta = \sqrt{\frac{\mu}{\rho}}$, where μ is shear modulus and ρ is density of the material of the shear beam. These parameters characterize the material from which the shear beam is made.

The wave equation in one dimensional (1D) space is

$$\rho \frac{\partial^2 U}{\partial t^2} = \frac{\partial \sigma}{\partial x} \tag{1}$$

where, $\sigma = \mu\varepsilon$ is shear stress and ε is shear strain (Fig. 1).

For establishing "marching in time" procedure, we need to reduce the order of Eq. (1) in a system of partial differential equations (PDE) of first order.

Taking $V = \frac{\partial U}{\partial t}$ and considering above stress-strain relation, the Eq. (1) reads

$$\frac{\partial V}{\partial t} = \frac{1}{\rho}\frac{\partial}{\partial x}(\mu\varepsilon) \tag{2}$$

If we differentiate both sides of identity $\frac{\partial U}{\partial t} = \frac{\partial U}{\partial t}$ with respect to *x* and change order of differentiation of left and right side, we get:

$$\frac{\partial}{\partial t}\left(\frac{\partial U}{\partial x}\right) = \frac{\partial}{\partial x}\left(\frac{\partial U}{\partial t}\right) \tag{3}$$

Substituting $\varepsilon = \frac{\partial u}{\partial x}$, taking into account definition of vend plugging in Eq. (3) we get:

$$\frac{\partial \varepsilon}{\partial t} = \frac{\partial V}{\partial x} \tag{4}$$

On this way the original second-order wave equation is reduced on system of two first-order PDEs:

$$\frac{\partial V}{\partial t} = \frac{\mu}{\rho}\frac{\partial \varepsilon}{\partial x} \tag{5}$$

$$\frac{\partial \varepsilon}{\partial t} = \frac{\partial V}{\partial x} \tag{6}$$

Suitable for establishing of "marching in time" procedure.

Eqs. (5) and (6) in vector form are:

$$\{U\}_{,t} = \{F\}_{,x} \tag{7}$$

where, $\{U\} = \begin{Bmatrix} V \\ \varepsilon \end{Bmatrix}$ and $\{F\} = \begin{Bmatrix} \frac{\mu\varepsilon}{\rho} \\ V \end{Bmatrix}$.

Dirichlet boundary condition implies zero displacements. The allowable shape of 1D beam with applied Dirichlet boundary conditions at both ends is presented on Fig. 2a. The time history of the displacement at arbitrary point of the beam under forced vibrations is presented on Fig. 2b.

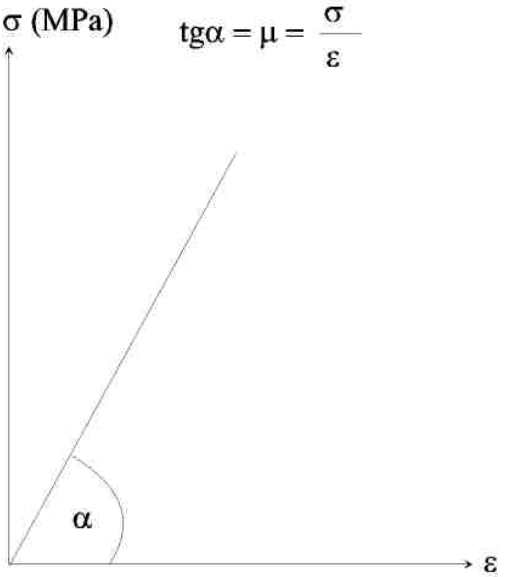

Fig. 1 Linear stress-strain dependence.

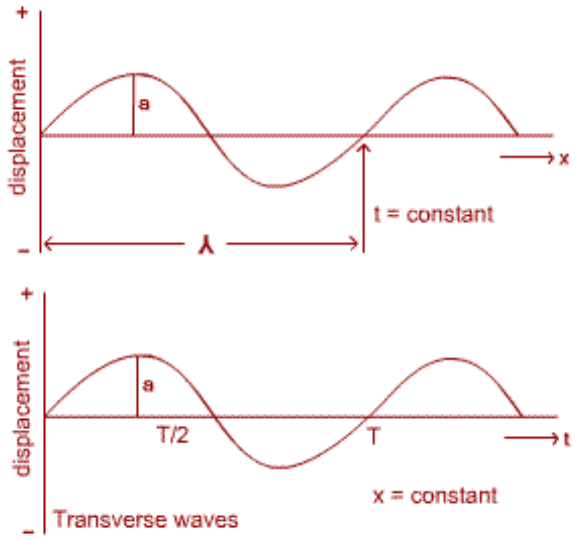

Fig. 2 Allowable motion of a beam with applied fixed boundary conditions at both ends. (a) Shape of deformed beam in arbitrary time instant; (b) Time history at arbitrary point of the beam.

3. Numerical Examples

We consider a beam with height H = 50 m, divided on 200 equal space intervals. Wave with half-sine form is generated at bottom end (x = 0) and starts to propagate along the beam towards the top. Velocity of propagation of the wave is 300 m/s, the amplitude of the pulse is A = 0.1 m, and duration of the pulse is t_d = 0.1 s (Fig. 3).

After applying the pulse at the bottom ($t > t_d$), the bottom end remains motionless, e.g. fixed Dirichlet boundary condition is prescribed at the bottom end. While the pulse occupies a point of the beam, its displacement is:

$$u = a \cdot sin\frac{\pi t}{t_d} \tag{8}$$

where, $a = 0.1$ m is amplitude and $t_d = 0.1$s is duration of the pulse.

Differentiating Eq. (8) with respect to time, we get the particle velocity which for our example is:

$$\frac{\partial u}{\partial t} = v = \frac{a\pi}{t_d} \cdot cos\frac{\pi t}{t_d} = \frac{0.1\pi}{0.1} cos\frac{\pi t}{t_d} \xrightarrow{yields} v_{max} = \frac{0.1\pi}{0.1} = \pi \tag{9}$$

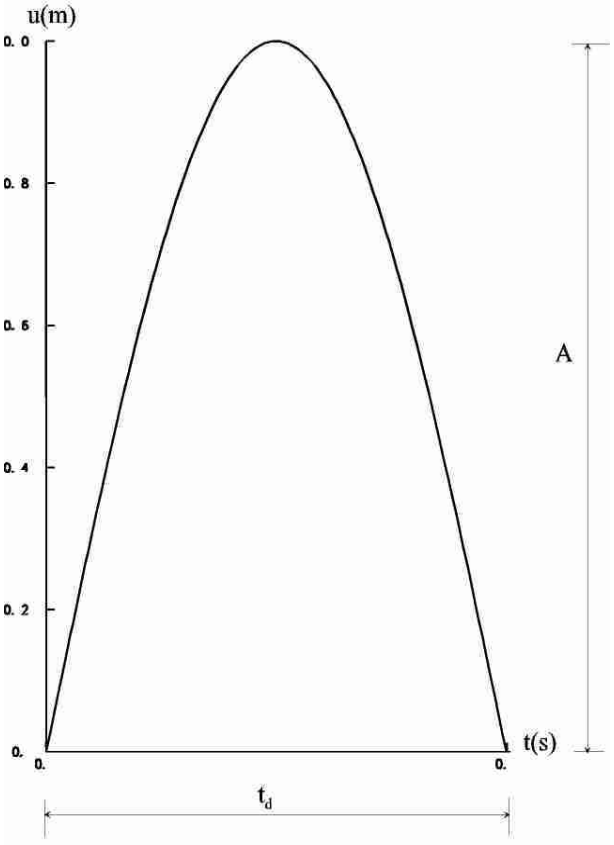

Fig. 3 Incident wave with half-sine waveform.

To obtain the strain, we multiply and divide the argument of sine function in Eq. (8) by velocty of propagation:

$$u = a \cdot sin\frac{\pi t\beta}{t_d\beta} \tag{10}$$

Taking that $\beta t_d = L$ is length of the pulse and $\beta t = x$ is spatial coordinate along the length of the pulse, Eq. (10) becomes:

$$u = a \cdot sin\frac{\pi x}{t_d\beta} \tag{11}$$

Differentiating Eq. (11) with respect to x, we get the strain:

$$\frac{\partial u}{\partial x} = \varepsilon = \frac{\pi a}{t_d\beta} \cdot cos\frac{\pi x}{t_d\beta} \xrightarrow{yields} \varepsilon_{max} = \frac{\pi a}{t_d\beta} = \frac{v_{max}}{\beta} = \frac{\pi}{\beta} \tag{12}$$

If $\beta = 300$m/s, the maximum value of the strain is $\varepsilon_{max} = \frac{\pi}{\beta} = \frac{\pi}{300} \sim 0.01$ what can be seen also from our numerical results in Figs. 4c1 and 4c2.

3.1 Results

On following figures, we presented the results obtained by numerical simulation of the propagation of wave in form of half-sine pulse (Fig. 3).

On Fig. 4 the response of the point at the middle of the beam (point 100, x = H/2 = 25 m) is shown. The response is shown via displacements u, particle velocities, v, and strains ε at that point versus time, t. On left side of Fig. 4 we show the response for fixed boundary, $u = 0$, at the top x = H = 50 m (Dirichlet, Figs. 4a1, 4b1 and 4c1), while on the right side the response for stress-free boundary, $\varepsilon = \frac{\partial u}{\partial x} = 0$, at the top (Neumann, Figs. 4a2, 4b2 and 4c2) is shown.

Comparing displacements (Figs. 4a1 and 4a2) it can be noticed that in case of fixed (Dirichlet) boundary at top, after reflection the pulse changes sign and it comes in the middle of the beam (point 100) with opposite (negative) displacement than in the first passage through that point (second peak on Fig. 4a1 is with negative sign). In case of free-stress (Neumann) top boundary after reflection from the top the pulse does not change the sign and it comes at the point 100 with same (positive) displacements as in the first passage. The situation is the same with particle velocity (half-cosine pulse, Figs. 4b1 and 4b2).

Dislike displacements and particle velocities, the strains, ε, after reflection from the fixed (Dirichlet) top does not change sign (all half-cosines on Fig. 4c1 start with negative and finish with positive signs). For stress-free (Neumann) top end, after reflection the strains change signs (Fig. 4c2). So, if we analyze Fig. 4c2, we can notice that the first half-cosine pulse going upward passing through point 100 starts with negative values, while after reflection from the top it changes sign and comes at point 100 with opposite values (first positive and then negative). Then it reflects from bottom end (Dirichlet), does not change sign, so the third half-cosine is the same as second, then it reflects from top (Neumann), changes sign so the fourth half-cosine is opposite of third etc. One can learn from the above analysis that fixed end (Dirichlet boundary condition) changes sign of the displacement, u and particle velocity, v, while it does not change sign of strain, ε after reflection. Opposite, stress-free (Neumann boundary condition) does not change sign of displacements, u, and particle velocities, v, while it changes sign of the strains, ε, after reflection. Common for both boundary conditions is that after multiple reflections, the amplitudes of the pulse are the same (in absolute values). The above analysis is summarized on Fig. 5. It is a 3D view of displacement of the shear beam versus scaled, dimensionless time and space.

In the real world, dislike the fixed (Dirichlet) boundary at the bottom, the structures are not fixed in the ground (zero motion), but rather there is some nonzero motion (moving boundary) at the bottom during the passage of the wave through soil-structure interface. Also the real structures, at the top end are not bounded and can freely move (Neumann boundary condition).

Response of such a structure analized with 1-D shear beam model is shown on Fig. 6. At top row (Figs. 6a1, 6b1 and 6c1) the displacement, particle velocity and strain at the middle of the beam, $x = H/2$ = 25 m (point 100), vs. time are presented. Comparing Figs. 4a2, 4b2 and 4c2 with Figs. 6a1, 6b1 and 6c1 one can notice that the shape is the same (in both sets at the top there is stress-free, Neumann boundary condition). The differences are boundary conditions at bottom. While the Figs. 4a2, 4b2 and 4c2 show the response for fixed bottom boundary, the Figs. 6a1, 6b1 and 6c1 show the response of the beam for moving bottom boundary. The moving boundary is a type of Dirichlet boundary which prescribes motions, not derivatives of motions like Neumann boundary and that is the reason why Figs. 6a1, 6b1 and 6c1 resemble Figs. 4a2, 4b2 and 4c2 in shape. Only at moving boundary is the motion not zero as in case of fixed boundary. As a consequence after each reflection from bottom, part of the wave energy is transmitted in the soil and only a part is being reflected back in the beam which propagates upward. On this

way, after each reflection from the bottom, the wave remaining in the beam (structure) is weakened.

In Figs. 6a2, 6b2 and 6c2 we can see the phenomenon of wave interference in point 150 close to the top (x = 3H/4 = 37.5 m). Part of the pulse going upward interferes with part of the pulse going downward and they add up. This is obvious at strains (Fig. 5c2) where the strain amplifies almost twice. This is the reason for generating high stresses $\sigma = \mu\varepsilon$ that can be reason for collapse of the structure.

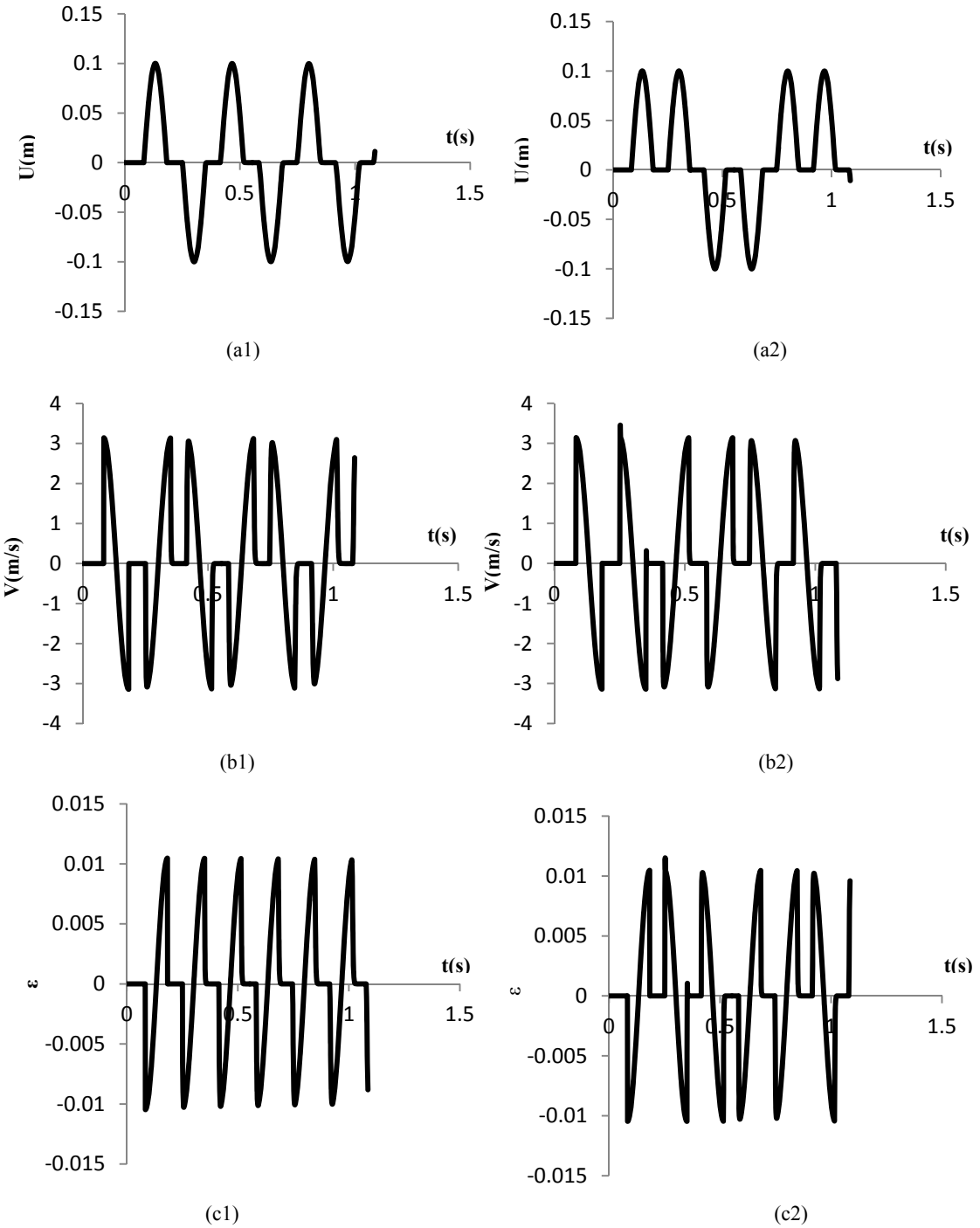

Fig. 4 Displacement, particle velocity, and strain at x = H/2 vs. time for β = 300 m/s, Dirichlet (a1, b1 and c1) and Neumann (a2, b2 and c2) boundary conditions.

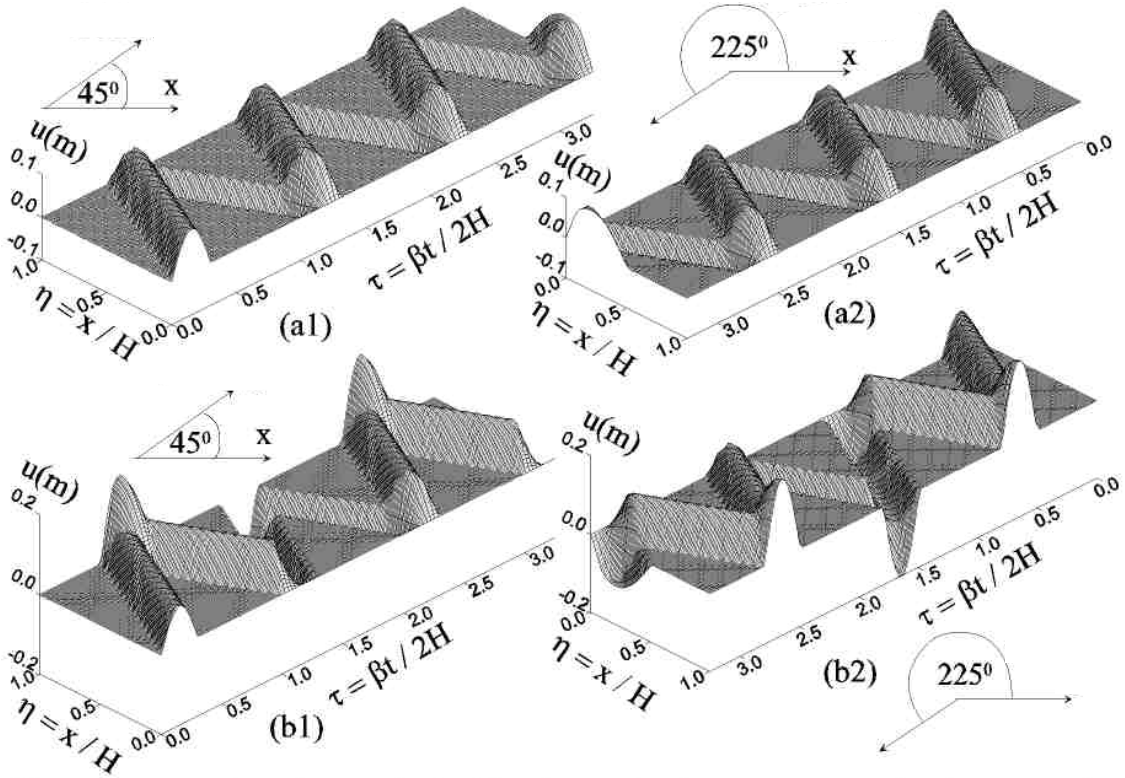

Fig. 5 Displacement of the beam as a function of dimensionless time t and dimensionless height η for two view angles. Dirichlet (a1 and a2) and Neumann (b1 and b2) boundary conditions.

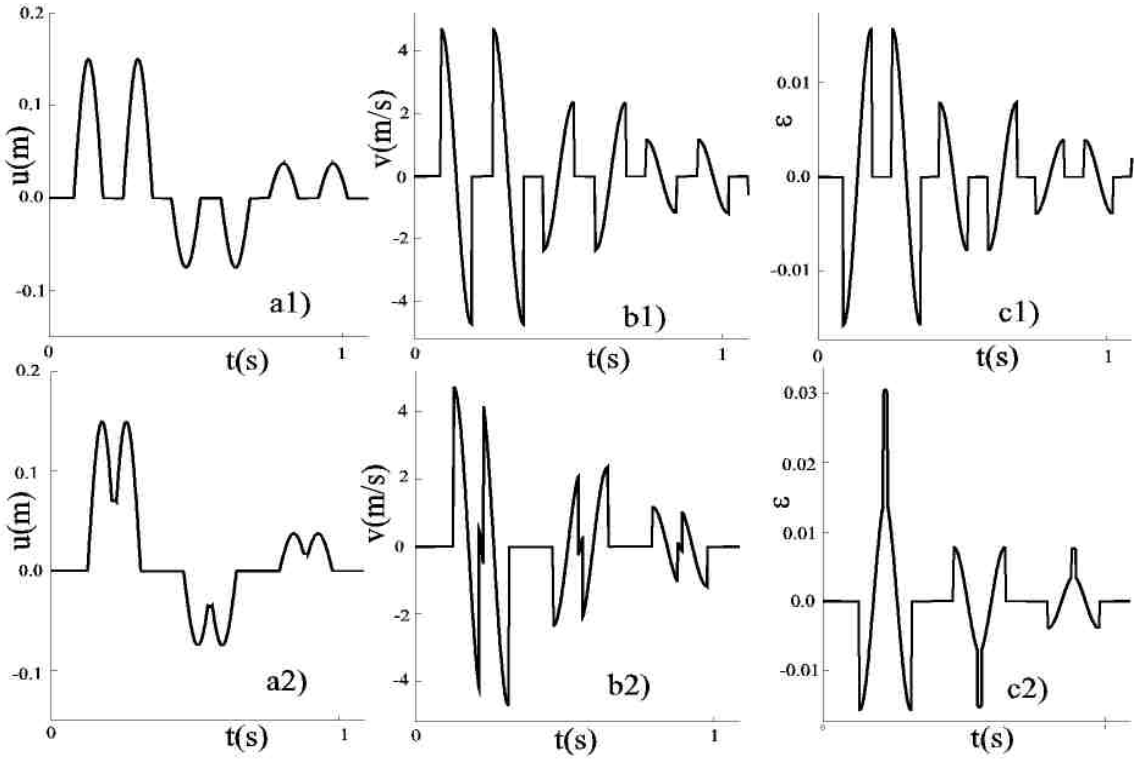

Fig. 6 Displacement, particle velocity, and strain in case of moving boundary at bottom and stress-free boundary at top.
a1, b1 and c1 at $x = H/2$ (point 100);
a2, b2 and c2 at $x = 3H/4$ (point 150).

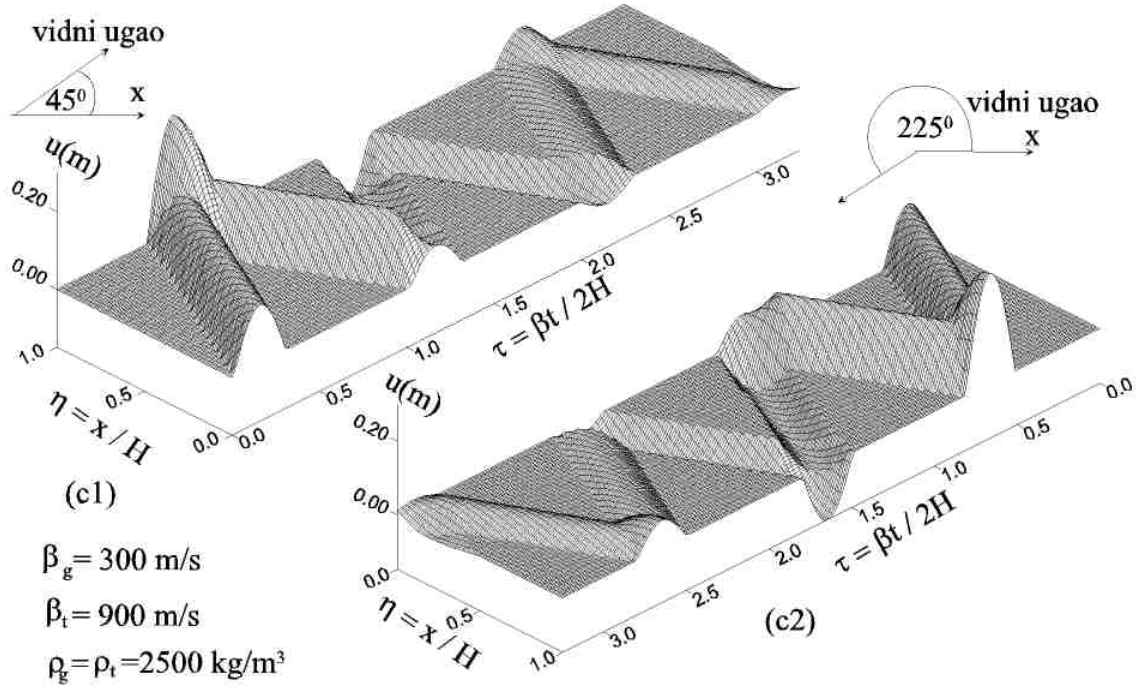

Fig. 7 Displacement of the beam versus dimensionless time, τ, and dimensionless height, η, for two view angles. Moving (realistic) boundary on soil-structure interface ($\eta = 0$). Characteristic points: $\eta = 0$: soil-structure interface (moving boundary), $\eta = 1$: top of the beam (structure), Neumann (stress-free) boundary condition.

Finally, on Fig. 7, a 3-D view of propagation of the the wave versus dimensionless time, τ, and dimensionless space, η, is presented. As can be seen from Fig. 7, after each passing of the wave through soil-structure interface, the reflected wave in the beam is weaker as a consequence of transmitting of the wave energy in the soil. The ratio of the reflected and transmitted wave depends upon the physical properties of the soil and structure and can be determined through reflection, k_r, and transmision coeficient, k_t [10].

4. Conclusions

Fixed end (Dirichlet boundary condition) changes sign of displacement, u and particle velocity, v, while it does not change sign of the strain, ε, after reflection. Opposite, stress-free (Neumann boundary condition) does not change sign of displacement, u, and particle velocity, v, while it changes sign of the strain, ε, after reflection. Common for both boundary conditions is that after multiple reflections, the pulse amplitudes are unchanged. For moving boundary at soil-structure interface, after each passage of the wave through it, the reflected wave remaining in the structure is attenuated, indicating that part of the energy is refracted in the soil. The ratio of the reflected and refracted wave depends on the physical properties of the soil and the structure can be determined with the coefficients of reflection and transmission.

References

[1] Fujino, Y., and Hakuno, M. 1978. "Characteristics of Elasto-Plastic Ground Motion during an Earthquake." *Bull Earthquake Res. Inst. Tokyo Univ.* 53: 359-78.

[2] Tsynkov, S. V. 1998. "Numerical Solution of Problems on Unbounded Domains. A Review." *Applied Numerical Mathematics* 27 (4): 465-532.

[3] Gicev, V., and Trifunac, M. D. 2010. "Amplification of Linear Strain in a Layer Excited by a Shear-Wave Earthquake Pulse." *Soil Dynamics and Earthquake Engineering* 30 (10): 1073-81.

[4] Gicev, V., and Trifunac, M. D. 2006. *Non-linear Earthquake Waves in Seven-Storey Reinforced Concrete Hotel.* Univ. of Southern California, Civil Eng. Dept. Report CE 06-03, available on: www.usc.edu/dept/civil_eng/Earthquake_eng/CE_Reports/CE_Reports.html.

[5] Gicev, V., and Trifunac, M. D. 2009. "Transient and Permanent Shear Strains in a Building Excited by Strong

Earthquake Pulses." *Soil Dynamics and Earthquake Engineering* 29 (10): 1358-66. Published Online: Jun 3 2009, DOI: 10.1016/j.soildyn.2009.05.003.

[6] Safak, E. 1998. "New Approach to Analyzing Soil-Building Systems." *Soil Dynam. and Earthquake Eng.* 17: 509-17.

[7] Trifunac, M. D. 2006. "Effects of Torsional and Rocking Excitations on the Response of Structures." In *Earthquake Source Asymmetry, Structural Media and Rotation Effects*, edited by Teisseyre, R., Takeo, M., and Majewski, E. Heidelberg, Germany: Springer.

[8] Gicev, V., and Trifunac, M. D. 2007. "Permanent Deformations and Strains in a Shear Building Excited by a Strong Motion Pulse." *Soil Dynamics and Earthquake Engineering* 27 (8): 774-92.

[9] Kausel, E., and Tassoulas, J. L. 1981. "Transmitting Boundaries: A Close-Form Comparison." *Bull. of the Seismological Society of America* 71 (1): 143-59.

[10] Gicev, V. 2005. "Investigation of Soil-Flexible Foundation-Structure Interaction for Incident Plane SH Waves." Ph.D. Dissertation, Univ. of Southern California, Los Angeles, CA.